AIAA JOURNAL
Vol. 47, No. 11, November 2009

Variable-Frequency Fluidic Oscillator Driven by a Piezoelectric Bender

James W. Gregory*
The Ohio State University, Columbus, Ohio 43235
Ebenezer P. Gnanamanickam† and John P. Sullivan‡
Purdue University, West Lafayette, Indiana 47907
and
Surya Raghu§
Advanced Fluidics, LLC, Ellicott City, Maryland 21042

DOI: 10.2514/1.44078

A new actuator for aerodynamic flow control applications is described and evaluated in this paper: the piezo-fluidic oscillator. This actuator is a fluidic device based on wall attachment of a fluid jet and modulated by piezoelectric devices. The piezo-fluidic oscillator successfully decouples the operating frequency from the flow characteristics of the device. The frequency is specified by an input electrical signal that is independent of pressure, making this actuator ideal for closed-loop flow control applications. The oscillator exhibits high bandwidth (up to 1.2 kHz), modulation rates up to 100%, and a velocity range reaching sonic conditions. Furthermore, the bistable actuator may be operated in a steady state, with momentum flux in one of two desired directions for flow vectoring purposes. The piezo-fluidic oscillator may be used in flow control applications in which synthetic jets or plasma actuators cannot provide enough momentum for control authority. This paper details the design and characterization of the piezo-fluidic oscillator. The dynamic response characteristics are evaluated with flow visualization and hot-film probe measurements on the output.

I. Introduction

FLOW control is a rapidly developing field in applied fluid dynamics, with much of the work focused on actuator development, sensor systems, control logic, and applications. Flow control actuators are devices that are used to enact large-scale changes in a flowfield. Often these changes are focused on improving the performance of a flight vehicle: by delaying stall, reducing drag, enhancing lift, abating noise, reducing emissions, etc. In many flow control situations, unsteady actuation is required for optimal performance. Unsteady actuators are particularly beneficial in closed-loop control applications when the unsteady actuation can be controlled and synchronized with characteristic time scales of the flowfield. Common flow control actuators include synthetic jets [1], piezoelectric benders for direct excitation [2,3], powered resonance tubes (also known as Hartmann whistles) [4–6], plasma actuators [7–9], pulsed combustion actuators [10–12], pulsed jets [13,14], and steady blowing [15] or suction [16]. These devices and concepts all have inherent strengths and some limitations. Thus, the selection of a flow control actuator is often driven by the requirements of the application.

The ideal actuator will have a high-frequency bandwidth and direct control by an electrical signal for closed-loop applications. The device should be simple and robust for reliable flight operations: devices with few moving parts are desirable for mechanical reliability. The ideal actuator should also be capable of a large range of flow rates, but should only provide enough momentum input for sufficient control authority. Some applications require large flow rates that current actuators cannot deliver. Jet thrust vectoring on a flight vehicle is one such example. Miller et al. [17] and Yagle et al. [18] specified that the ideal actuator for this application is a pulsed jet that operates at 1 kHz with 100% modulation of the jet at sonic conditions. The focus of the present work is on the development of a fluidic oscillator toward the following design goals: high bandwidth, high mass flow rates, and an operating frequency that is decoupled from the flow rate.

The fluidic oscillator is a device that generates an oscillating or pulsed jet when supplied with a pressurized fluid, as shown in Fig. 1. The development history of fluidic oscillators is very rich and extensive, being grounded in the field of fluidic amplifiers [19–22]. Typical oscillators are bistable devices that operate on the principle of wall attachment, as shown in Fig. 2. When a free jet of fluid is adjacent to a wall, entrainment of flow around the jet causes a low-pressure region between the wall and the jet that draws the jet closer to the wall. Thus, the jet will deflect until it has attached to the wall. This principle was observed by Coanda [23] in the 1930s and was later named the Coanda effect [24]. Coanda [23] originally appropriated this phenomenon for steering streams of fluid.

If there are two adjacent walls, such as the symmetric configuration shown in Fig. 2, the jet will arbitrarily attach to one wall or the other, based on random disturbances in the flow. Traditional fluidic devices employ a control port at the nozzle, where injected mass flow can force the jet to detach from the wall and reattach to the opposite wall. This occurs through the creation of a separation bubble between the jet and the wall. As more fluid is injected from the control port, the separation bubble enlarges and extends downstream until the jet has entirely separated. The pressure differences and momentum of this separation process then carry the jet over to the opposite wall, where it reattaches. The primary advantage of this arrangement is that the

Presented as Paper 108 at the 43rd AIAA Aerospace Sciences Meeting and Exhibit, Reno, NV, 10–13 January 2005; received 28 February 2009; revision received 14 July 2009; accepted for publication 16 July 2009.

*Assistant Professor, Department of Aerospace Engineering, Aeronautical/Astronautical Research Laboratory, 2300 West Case Road; gregory.234@osu.edu. Senior Member AIAA.

†Graduate Research Assistant, School of Aeronautics and Astronautics, 701 West Stadium Avenue. Student Member AIAA.

‡Professor, School of Aeronautics and Astronautics, 701 West Stadium Avenue. Associate Fellow AIAA.

§President, 4217 Red Bandana Way. Associate Fellow AIAA.

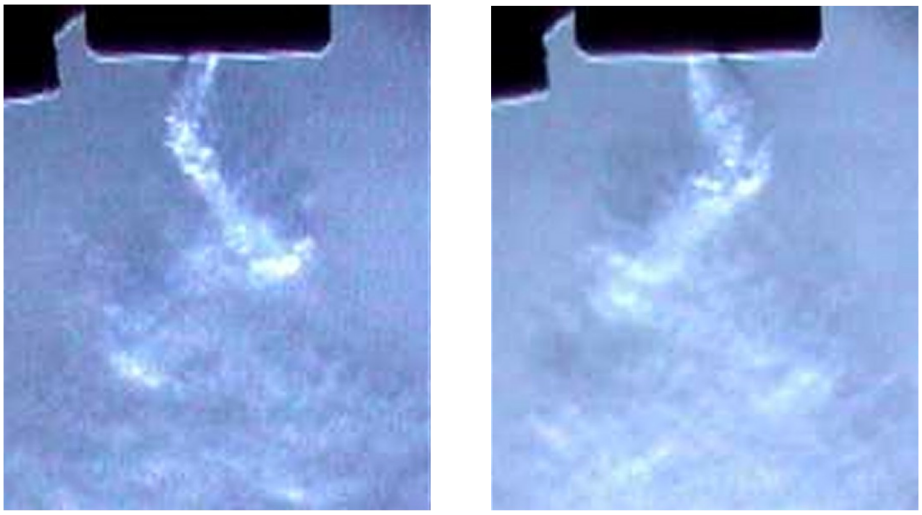

a) b)

Fig. 1 Schlieren images illustrating the typical flowfield of a fluidic oscillator at two phase positions within the oscillation cycle, relative to an arbitrary trigger point: a) 0 deg and b) 180 deg.

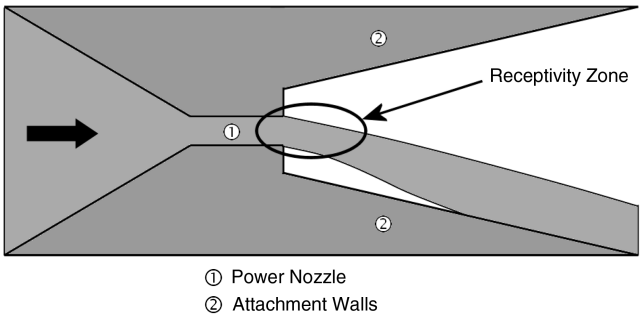

Fig. 2 The principle of wall attachment in a fluidic device, known as the Coanda effect.

device serves as a fluid amplifier: the effects of the control flow at the control ports can be amplified by an order of magnitude to affect the exiting jet flow. Thus, the momentum of the modulated input is amplified to create a higher-momentum modulated output.

If the two control ports on a fluidic device are set up with a feedback loop system, with input to the feedback loops provided by a small portion of the jet exit flow, then the fluidic device can create self-sustained oscillations. When the primary jet is attached to a given wall, a portion of that jet is transmitted back to the control port on that side through a feedback tube. This control flow causes the jet to switch to the opposite attachment wall, where the same process occurs. Thus, self-sustaining oscillations are created by the feedback system, which is the typical arrangement of many fluidic oscillators. The disadvantage of this configuration, however, is that the frequency of oscillations is directly coupled to the flow rate through the device, as shown clearly by Viets [19].

Fluidic oscillators have been used in many diverse applications, such as windshield washer fluid nozzles [25] and flow rate metering [26–28]. There has also been a recent surge in interest for using fluidic oscillators for flow control applications. Raman et al. [29] and Raghu and Raman [30] used the oscillators for applications such as cavity resonance tone suppression, jet thrust vectoring [31], and enhancement of jet mixing [32,33]. More recently, Gregory et al. [34] have focused on understanding the internal fluid dynamics of feedback-free fluidic oscillators and developing them for flow control applications. The feedback-free configuration of fluidic oscillator operates based on the interaction of two jets in an internal mixing chamber versus the traditional configuration of feedback tubes influencing the primary jet via control ports. Gregory et al. [35] also characterized a microscale feedback-free fluidic oscillator, which has very low mass flow requirements, making it highly suitable for flow control applications. Tesar et al. [36,37] and Tesar [38] recently developed fluidic actuators that provide suction and blowing in a manner similar to a synthetic jet. Arwatz et al. [39] also developed a fluidic actuator that provides pulsatory suction and blowing. Lucas et al. [40] recently reported the application of fluidic oscillators for airfoil separation control and download alleviation on a V-22 wing. Cerretelli and Gharaibah [41] conducted investigations of the physical operation of fluidic oscillators, along with application of fluidic oscillators to separation control on airfoil sections for wind turbine flow control [42].

Conventional fluidic actuators have a significant limitation when used for flow control: the oscillation frequency is directly dependent on the flow rate through the device. For practical flow control problems, however, it is highly desirable to decouple the operating frequency from the flow rate of the actuator. This is the motivation for developing a piezoelectric-driven fluidic oscillator. This concept has been used with some success in the past to develop a bistable electrofluidic pneumatic valve for fluid amplifier technology. Miller [43] originally proposed using piezoelectric devices for fluidic control, in which a double-clamped piezoelectric bender was used to produce acoustic signals for fluidic control. As such, the pressures produced by the piezo bender were very low ($\sim$100 Pa) and even a high-gain fluidic amplifier would have a marginal output. Despite the low-pressure output, Miller demonstrated operation of the device up to 1 kHz. Tesar [44] demonstrated the use of a ferromagnetic filament to guide a jet of air or water in various directions through the Coanda effect. The deflection of the filament was controlled by an adjacent electromagnet. Tesar's demonstrations were confined to low-frequency deflections (68 Hz) at low pressures. Tesar also briefly suggested the use of filaments with an electrostatic charge, as well as piezoelectric benders for jet control. Taft and Herrick [45,46] used a piezoelectric bender to alternately block the input to either one of the two control ports on a fluidic device. They operated the device in an unsteady mode and recorded a flat frequency response up to about 40 Hz with a corresponding phase shift of 90 deg [45]. In later work they demonstrated a flat frequency response of 1 kHz with this same device [46]. Chen and Lucas [47] and Chen [48] developed a monostable fluidic injector with a piezo bender on the unstable side control port. Chen's work focused on developing the device as a fuel injector for natural gas engines, for which switch-on response times of 1.65 ms and switch-off response times of 1.85 ms were achieved. Within the context of fluidic oscillators applied to flow control applications, Gregory et al. [49] first presented the concept of decoupling frequency from flow rate through the use of piezoelectric devices, which is the basis for the current work. In a separate

investigation on the development of frequency-independent fluidic actuation, Gregory et al. used dielectric barrier discharge plasma actuators in the control ports to force the driving frequency at rates independent of the flow rate [50]. Culley [51] and Feikema and Culley [52] also recently reported a similar frequency-independent investigation in which small fast-acting valves were coupled to the control ports to drive the switching process.

Many of the existing actuators lack the combination of high bandwidth and high mass flow rates. The work presented in the current paper details the development of a piezo-driven fluidic oscillator for use as a flow control actuator. A bistable wall-attachment fluidic oscillator is used along with piezoelectric transducers to achieve oscillatory or steady-state control flow. The piezo-fluidic oscillator successfully decouples the operating frequency from the supply pressure to the device. The actuator can deliver the high mass flow rates that are demanded in some flow control applications. Furthermore, the device is shown to have a wide bandwidth, with partial frequency coverage from 0 to 1.2 kHz. The actuator performance is characterized through flow visualization studies and hot-film probe measurements.

II. Piezo-Fluidic Oscillator Design Concepts

The main concept of the piezo-fluidic oscillator is the modulation of a fluid jet by piezoelectric transducers. There are many possible realizations of this concept, which are described as follows. In all cases, the piezoelectric transducer creates a geometrical or fluid dynamic asymmetry in a receptive location in the flowfield. The area of maximum receptivity is just downstream of the power nozzle (as shown in Fig. 2), where a traditional fluidic oscillator's control ports are typically located. One concept employs piezoelectric buzzers coupled to the control ports in a manner similar to Miller's design [43]. The challenge with this design is that a high level of acoustic energy is needed to reach the jet switching threshold of a practical device. This design was attempted in the early stages of this work, but was later abandoned due to insufficient control authority of the piezo buzzers. A similar iteration on this concept would employ synthetic jets at the control ports.

Other concepts employ piezoelectric benders or extenders to change the geometry of the device. A small asymmetry in the power nozzle region can readily cause the jet to switch to the opposite sidewall. A single piezoelectric bender may be positioned on the jet centerline, with the oscillating end pointing either upstream or downstream in the flow. The oscillatory motion of the bender will cause deflection and switching of the jet between the two sidewalls. Another concept is to use piezoelectric benders or extenders in lieu of the control ports. When two extenders are driven 180 deg out of phase from one another, a geometric asymmetry is created in the shear layer of the jet, causing the jet to attach to the alternate sidewalls. A final concept involves a monostable oscillator with only one attachment wall and a piezoelectric bender mounted flush on the attachment wall with the free end pointing upstream into the jet. As the transducer is modulated, the tip will be either flat against the wall or facing into the flow such that the jet detaches from the wall. In the monostable configuration, the unstable location is a free jet that is unattached to an adjacent sidewall.

The design evaluated in this paper is based on a cantilevered piezoelectric bender pointed upstream into the nozzle, as shown in Fig. 3. This configuration was selected because it provided the best modulation characteristics of the jet flow and the best frequency response. The power nozzle in this geometry is 0.5 mm wide and about 5.5 mm high, with an adjacent wall angle of 30 deg. The piezoelectric bender employed in this configuration is a four-layer piezoceramic (T434-A4-302 from Piezo Systems, Inc.) that measures 72.4 mm long, 5.1 mm high, and 0.86 mm thick. The specified deflection of the device is $\cong$ 1050 μm with a resonant frequency of 121 Hz. The piezo bender was driven by a square wave signal from a function generator and amplified by a Lasermetrics voltage amplifier. The amplifier output was passed through an resistance–capacitance circuit to remove the dc bias on the supply. The resulting signal supplied to the piezo bender was a 40 Vrms square wave.

III. Measurement Techniques

Instrumentation systems involved in characterizing the fluidic oscillator were schlieren imaging, pressure-sensitive paint (PSP), and hot-film probes with a computer data acquisition system. The schlieren and PSP systems were used for flow visualization, and the hot-film probes were used for quantitative velocity and frequency measurements. These techniques were selected to understand the dynamics of the switching process and to evaluate the response characteristics of the actuator configuration. The experimental setup for the PSP and hot-film probe techniques is shown in Fig. 4. The piezo-fluidic actuator is oriented vertically in this image, with PSP instrumentation in front and behind the actuator and with hot-film probes oriented at the exit.

The schlieren imaging experimental setup involved the use of a single-pass schlieren system [53]. The illumination source was a strobe light (General Radio Company model 1538-A Strobotac). A neutral-density filter was placed in front of the strobe light to control the light intensity passing through the flow and reaching the camera. A 6-in.-diam. front-surface concave mirror with a focal length of 5 ft was used to pass the light through the flowfield. A knife edge was placed at the focal point of the mirror to improve the image contrast. The flowfield was then imaged with a Nikon D100 digital camera.

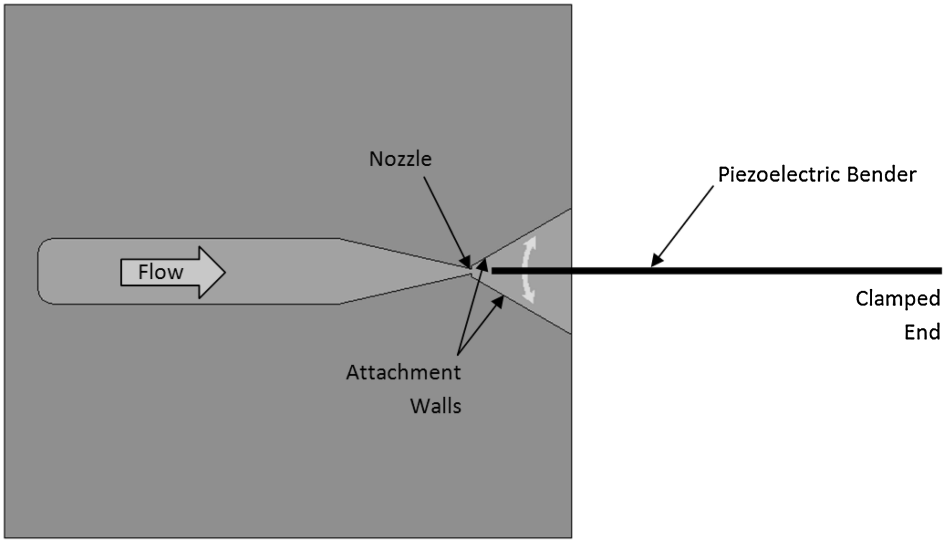

Fig. 3 Diagram of the piezo-fluidic actuator design. The piezoelectric bender is positioned in the diffuser, pointing upstream into the flow.

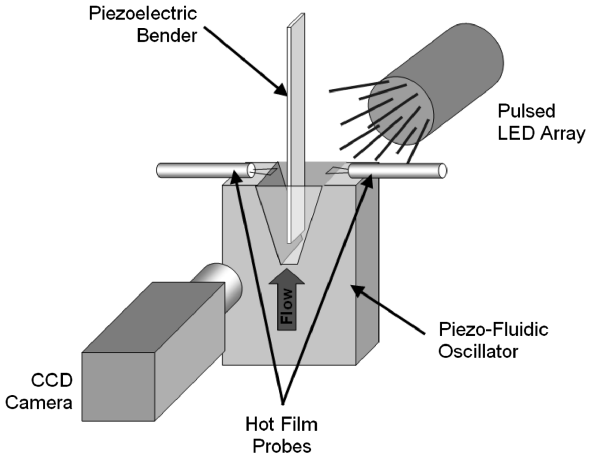

Fig. 4 Experimental setup for the pressure-sensitive paint and hot-film probe instrumentation.

Hydrogen gas was used with the oscillator to enhance the density contrast with ambient air.

PSP was used to visualize the internal fluid dynamics of the oscillator. PSP is an optical measurement tool for measuring surface pressures and is based on oxygen quenching of excited luminescent molecules. Comprehensive descriptions of the technique are given by Bell et al. [54] and Liu and Sullivan [55]. Recent work with PSP has extended the frequency response well beyond 20 kHz [56–59], such that the current unsteady tests at 50 Hz are straightforward. An actuator was constructed with optically clear cover plates on the top and bottom. One of the cover plates was painted with PSP on the interior surface, facing the flow (see Fig. 4), and the second cover plate was used for viewing the PSP. The paint sample was backilluminated with an light-emitting diode (LED) array emitting 473 nm light and was imaged from the front with a 14-bit charge-coupled-device camera with a 55 mm f2.8 Nikon macro lens. A 590 nm long-pass filter (Schott Glass OG590) blocked the excitation light from the image. The illumination from the LEDs was phase-locked with the driving frequency of the piezoelectric transducer. Phase-averaged data were acquired with the camera shutter open for a relatively long period (1–2 s), and the LED array was synchronously driven by the input signal for the piezoelectric bender. Successive delays were introduced to step the phase of data acquisition throughout the cycle of the piezo actuation. The pulse width for PSP illumination was set to 2.5% of the period, and the delay step was 5% of the period. One phase-averaged image was taken at each delay step, producing 20 equally-spaced images throughout the oscillation cycle. Nitrogen was used as the supply gas for the PSP tests to enable high-contrast visualization of the jet dynamics by purging away ambient oxygen present in air. Wind-on and wind-off images were used to calculate the intensity ratio presented for visualization.

Hot-film probes were positioned at the ends of both attachment walls to measure the velocity and frequency content of the exiting flow. The hot-wire probes were operated in constant-temperature mode using a controller/signal conditioner with a specified frequency response of 10 kHz. The data from the probes were recorded through a computer data acquisition system with a sampling rate of at least 500 times the driving frequency. Data were simultaneously sampled to record the input signal to the piezoelectric bender as well as the velocity signals from both hot-film probes. Measurement uncertainty for the hot-wire probe data is conservatively estimated to be ± 1 m/s, based on the rms error of the calibration-data curve fit (a bias error). The precision error was significantly less than this value due to high levels of repeatability in the experiments. Thus, the overall uncertainty in the velocity measurements is estimated to be ± 1 m/s.

IV. Results and Discussion

Results presented in this section involve flow visualization with schlieren and PSP techniques and velocity measurements at the exit plane with hot-film probes. The velocity data are used to evaluate the response of the piezo-fluidic oscillator at various operating conditions and to generate frequency maps and bode plots.

A. Flow Visualization

Schlieren imaging was used to characterize the external flowfield of the piezo-fluidic actuator. Two images of the schlieren results are shown in Fig. 5, with flow moving from left to right. Hydrogen gas was the supply fluid, providing higher-contrast schlieren images due to the high-density gradient between the hydrogen and ambient air. These images represent bistable operation of the device, with the piezoelectric bender removed for clarity. The fluid jet is attached to top wall for the first image and then switched to the opposing wall for the second image. These images represent the steady-state operation of the bistable device, but the oscillatory operation will be similar to the jet switches between the two stable attachment locations.

Pressure-sensitive paint was used to visualize the internal fluid dynamics of the unsteady switching process. This process is repeatable from cycle to cycle, allowing for the use of phase-locking methods in the PSP measurement system. The driving square wave for the piezo bender was used as the phase-locking signal for these measurements. A series of PSP images is shown in Fig. 6 to illustrate the switching process, with a 1 ms time step separating each image. For these tests, the oscillator was driven at 50 Hz (20 ms period) at a pressure ratio P/P_{atm} of 1.14, or 14.3 kPa gauge. In Fig. 6a, the jet is

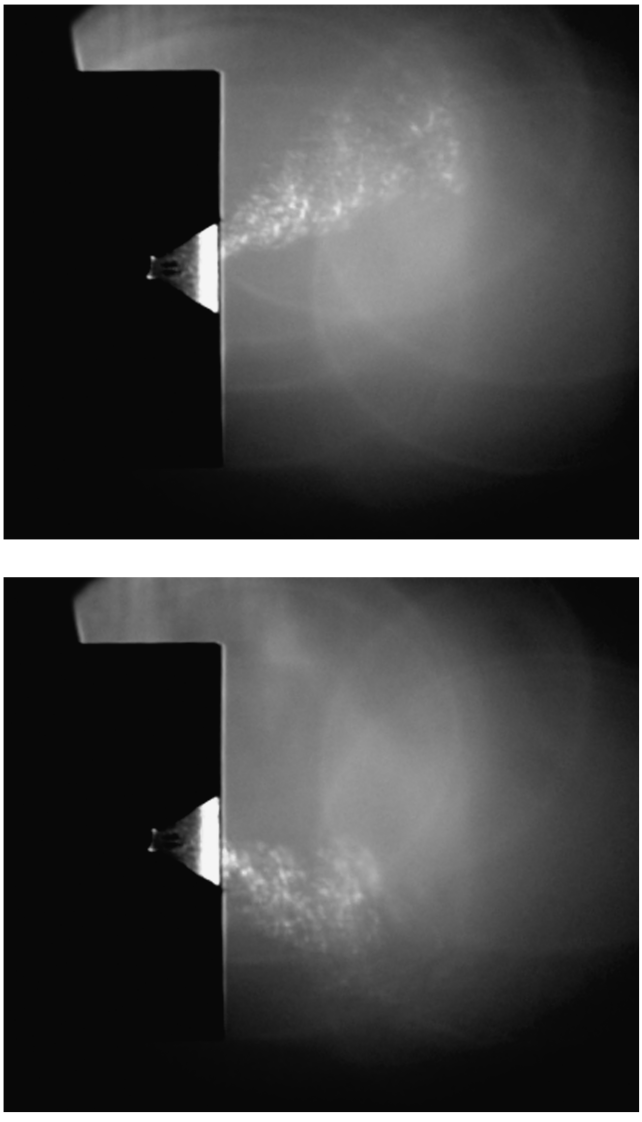

Fig. 5 Schlieren images of the bistable operation of the oscillator, with hydrogen gas used for visualization.

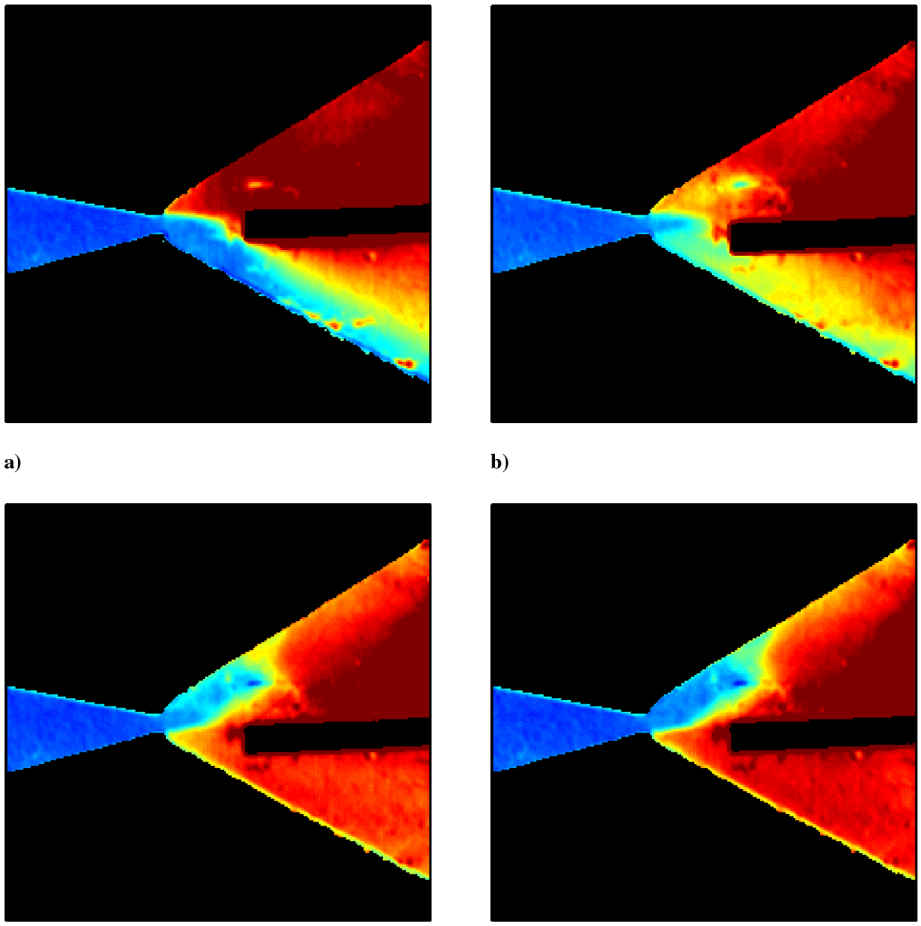

Fig. 6 Series of PSP visualization images with successive delays of 1 ms at an oscillation frequency of 50 Hz. Flow is from left to right, and the piezo bender coming from the right is shown in black. When the bender moves downward, it forces the jet to switch to the top attachment wall.

attached to the lower wall and flowing from left to right, and the piezo bender is near the centerline of the nozzle. As the bender moves downward in Fig. 6b, it creates a strong adverse pressure gradient in the jet and causes the jet to separate from the attachment wall. Within 1 ms, the jet has reattached to the opposing (upper) wall, because this location is more stable than the lower wall in the presence of the piezo bender. In image 6d the jet begins to convect downstream toward the exit of the oscillator (at the edge of the PSP image) and the piezo bender returns to the center location. These images represent one switching process (20% of the entire cycle), and two switches occur within each oscillation cycle.

B. Hot-Film Probe Data

The exit flow of the piezo-fluidic oscillator was characterized by simultaneous measurement of dual hot-film probes on either side of the device. Anticipated results should show that the two signals are 180 deg phase-shifted from one another and comparable in velocity magnitude. Temporal velocity data are presented in Fig. 7a at 10 Hz and Fig. 7b at 200 Hz for a pressure ratio P/P_{atm} of 1.69 (68.9 kPa gauge). Fluctuations in the velocity waveform are due to turbulent fluctuations as well as the directional ambiguity of the hot-film probes. The probes resolve not only the exit velocity of the flow, but also the switching velocity as the jet traverses across the exit plane. The summation of the two velocities produces the indicated output of the hot-film probe, an inherent limitation of the technique. The velocity signals for the low-frequency case show very little phase delay from the control signal, with very fast rise and decay times. The output of the oscillator at 200 Hz is phase-shifted approximately 180 deg from the low-frequency case (for reasons to be discussed later), but the modulation level remains quite high. This operating frequency is near the maximum for this modulation mode; however, another modulation mode emerges at higher frequencies to maintain operation to over 1 kHz.

The step response characteristics of the piezo-fluidic oscillator are shown in Fig. 8. A step input signal was sent to the piezoelectric bender, and the velocity response was recorded by a hot-film probe at the end of the adjacent attachment wall. The test was performed over a range of pressure ratios, and the response time was calculated. The step response times are summarized in Table 1. As should be expected, the response time decreases as the jet velocity increases. There is a finite amount of time required for the jet to convect from where it is switched at the control nozzle, down to the exit of the device. Because the convection time is related to the velocity of the jet, the higher velocities will produce a faster step response. The convection time is also related to the length of the attachment wall. If the wall length is decreased, the convection time would also decrease. These relationships indicate that the fastest step response time can be achieved with a high-velocity jet and the shortest possible wall length. Also note that the step response times for this geometry reach an asymptotic limit as the jet velocity is increased. This limit in the step response indicates that there are two time scales involved in the response: one due to the fluid convection time and the other due to delays in the electrical and mechanical switching time of the piezoelectric bender. The first time scale can be controlled by changing the jet velocity and wall length, and the second time scale can be controlled by changing the piezoelectric bender and driving circuitry. The magnitude of the piezoelectric bender step response time (approximately 2 ms, as shown in Fig. 8) is verified through comparison with the bender deflection time history observed in Fig. 6.

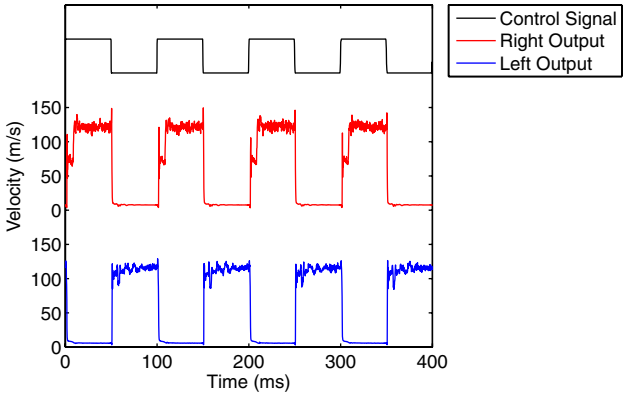

a)

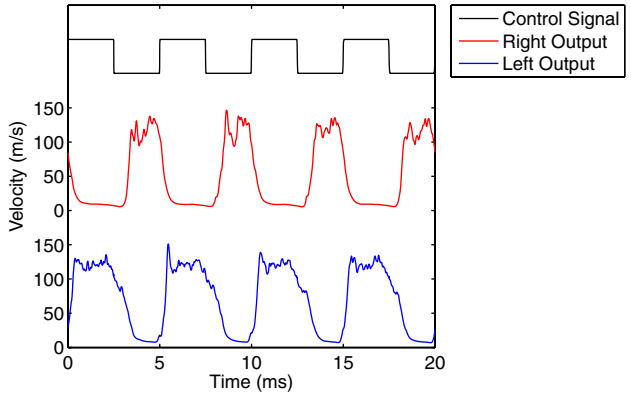

b)

Fig. 7 Time history of the oscillator outputs simultaneously measured by hot-film probes at a pressure ratio of 1.69: a) 10 Hz and b) 200 Hz.

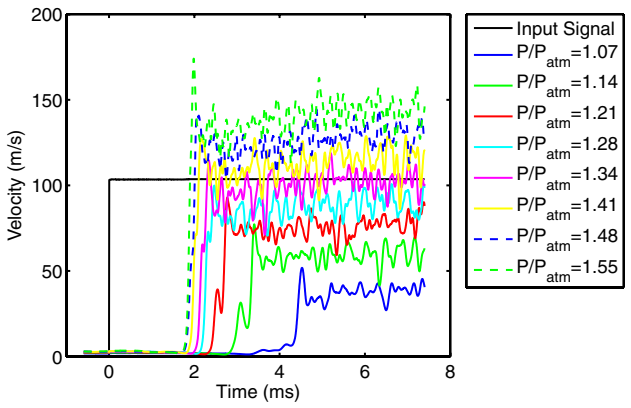

Fig. 8 Step response of the piezo-fluidic oscillator to the piezo bender. The response time decreases as the jet velocity increases.

Table 1 Summary of step response times

Pressure ratio	Response time, ms
1.07	4.52
1.14	3.41
1.21	2.78
1.28	2.47
1.34	2.34
1.41	2.16
1.48	2.06
1.55	1.99

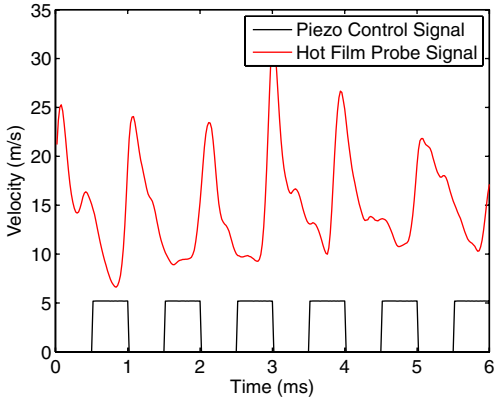

Fig. 9 High-frequency oscillations at 1.0 kHz and a pressure ratio of 1.14.

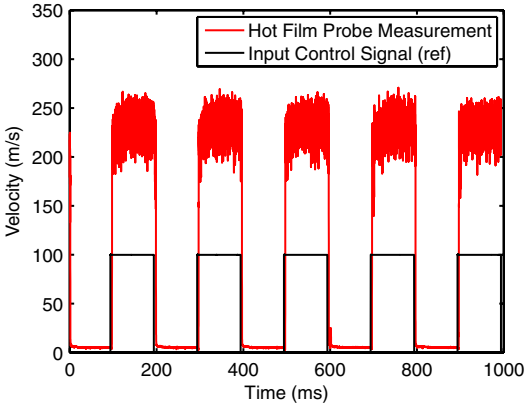

Fig. 10 Response of the piezo-fluidic oscillator at sonic nozzle conditions. The pressure ratio is 2.15 and the oscillation frequency is 5 Hz.

In addition to the continuous frequency coverage up to 200 Hz, the device is able to oscillate at frequencies in the kilohertz range. Figure 9 shows the response of the piezo-fluidic oscillator at a 1.0 kHz driving frequency and a pressure ratio of 1.14 (13.8 kPa gauge). The temporal velocity profile is no longer a square wave, but the jet is clearly modulated at the driving frequency. The piezo-fluidic oscillator also responds well at very high pressure ratios, as shown in Fig. 10. The pressure ratio for this case is 2.15 (115 kPa gauge), creating a sonic jet at the power nozzle. Despite the very high dynamic pressure loads on the piezoelectric bender, it is still able to modulate the jet at low frequencies (5 Hz).

Although the piezo-fluidic oscillator was operated at a pressure ratio of 1.14, the driving frequency was swept across a range from 0 to 1200 Hz to evaluate the bandwidth characteristics of the device. The low-frequency characteristics (0–250 Hz) are shown in Fig. 11a and the high-bandwidth characteristics are shown in Fig. 11b. Each vertical cross section of the figures is a typical power spectrum generated from the velocity measurements. Note that the primary frequency peak increases linearly with the driving frequency in a one-to-one relationship in both figures. For the low-frequency range, the first six or seven harmonics are clearly visible and increase linearly with the input frequency. The horizontal and vertical bands appearing in the spectra correspond to natural resonances of the piezoelectric bender in this flowfield. Figure 11b shows that the oscillator has a wide operating range from 0 to 1.2 kHz. There is a small region from 250 to 500 Hz in which the piezo bender appears unable to modulate the jet at this pressure. Within this region, the energy in the power spectrum shifts to the horizontal resonance line at 121 Hz. This indicates that the beam may be oscillating at its resonant frequency rather than the driving frequency in this range. At approximately 500 Hz, however, synchronous modulation resumes and increases linearly to the upper limit. The second and third harmonics are also visible at the higher driving frequencies.

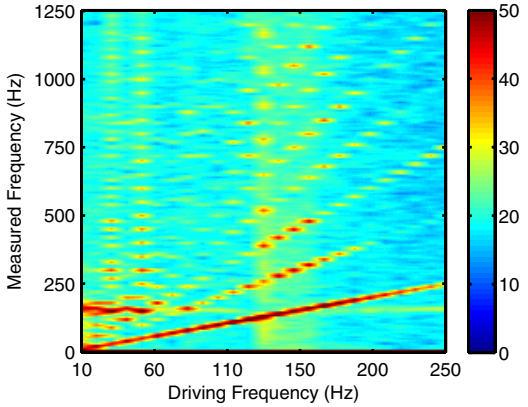

a)

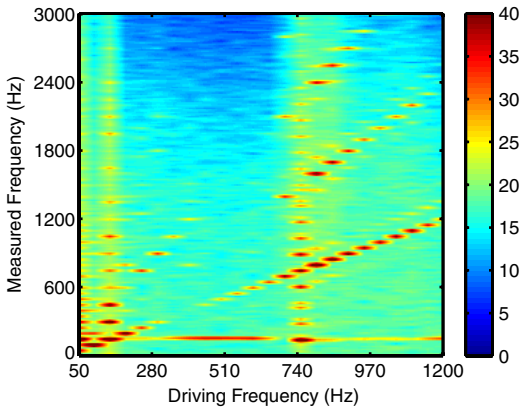

b)

Fig. 11 Frequency maps of the piezo-fluidic oscillator performance at a supply pressure ratio of 1.14. The ordinate indicates the driving frequency and the abscissa corresponds to the power spectral density.

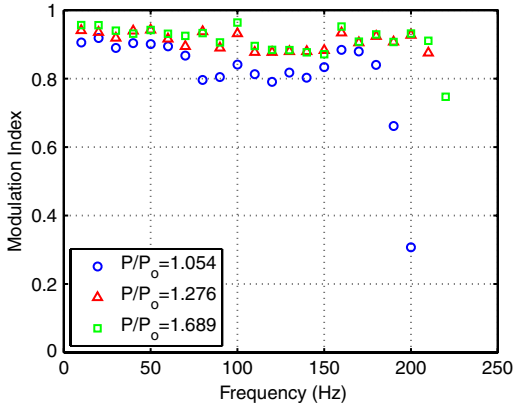

a)

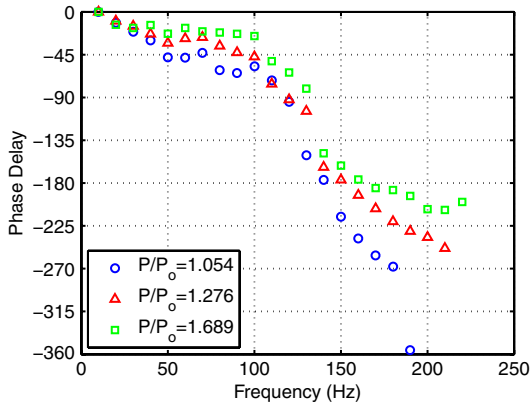

b)

Fig. 12 Plots of the piezo-fluidic oscillator response: a) magnitude and b) phase.

Magnitude and phase plots may be generated from the hot-film probe velocity data. The magnitude values are calculated from the modulation index M, which is defined as

$$M = \frac{V_{\max} - V_{\min}}{V_{\max} + V_{\min}} \tag{1}$$

where V is the measured velocity. A modulation index of 1 indicates that the jet is completely modulated from zero velocity up to its maximum value, making it a useful tool for identifying the level of modulation relative to any mean flow: an indication of how well the jet is turned on and off. The phase angle is defined as the delay between the control signal and the measured velocity at the exit of the actuator. This phase delay includes any electrical, mechanical, and fluid dynamic delays inherent in the system. Figure 12a shows data for the magnitude and Fig. 12b shows the phase for the actuator at three operating pressure ratios. The range of frequencies plotted here is limited to 250 Hz, where the modulation of the jet is clearly coherent with consistent phase characteristics. First, it is important to point out that the range of operating pressures has little effect on the response characteristics of the piezo-fluidic oscillator across this frequency range. The modulation index remains quite high (80 to 90%) across the entire range. The phase data show little roll-off until the resonance frequency of the bender is reached (121 Hz). The phase delay is less than 90 deg until this point, but then quickly rolls off beyond 180 deg. The modulation index remains roughly constant even after the break point in the phase delay, because the amplitude of the beam deflection remains high. Reasons for the increased phase delay are predominantly due to the mechanical and fluid response time scales. The piezoelectric beam takes a finite amount of time to move to a new deflection. As the modulation frequency increases, the proportion of this delay time relative to the oscillation period increases, causing an increase in the phase delay. The fluid response time scales, largely dependent upon the attachment wall length, also dictate the phase response characteristics of the flow output measured by the hot-film probes. For some applications, this phase delay is of no consequence, but for some closed-loop applications across a range of frequencies, it must be clearly characterized for compensation.

Further optimization of the device may be done to extend the operation envelope. The frequency bandwidth of the oscillator may be increased by selecting a piezo bender with a higher resonance frequency. Also, the length of the attachment walls may be shortened to decrease the convection time of the jet, thus increasing the maximum frequency. Piezoelectric beams with greater bending stiffness (more layers) may be used to control higher-momentum jets. Also, the location of the bender relative to the nozzle may be optimized for a particular operating point, to modulate the flow over a wider range.

V. Conclusions

The piezo-fluidic oscillator has been developed as a new type of flow control actuator. The oscillator can be driven directly by an electrical signal for closed-loop control applications and has successfully decoupled the oscillation frequency from the flow rate. The piezo-fluidic oscillator exhibits high bandwidth with a maximum operating frequency of 1.2 kHz at certain pressures. Over a range of 0 to 250 Hz, the oscillation frequency was nearly independent of supply pressure, and operation was maintained well beyond the piezo resonance frequency of 121 Hz. The modulation level remained constant near 90% across this frequency range, and the phase angle remained less than 90 deg until the piezo resonance frequency was reached. For oscillations at higher frequencies (500 to 1200 Hz), the jet is most likely modulated in some other manner by

the piezo bender, rather than by attachment to the adjacent walls. The piezo-fluidic oscillator was also successfully operated at sonic nozzle conditions at a frequency of 5 Hz. This new flow control actuator may be used for applications in which directed, high-momentum, frequency-controlled actuation is required.

Acknowledgments

This work was funded in part by the NASA Graduate Student Researcher's Program. The authors thank The Boeing Company for the loan of a charge-coupled-device camera used in this work.

References

[1] Glezer, A., and Amitay, M., "Synthetic Jets," *Annual Review of Fluid Mechanics*, Vol. 34, 2002, pp. 503–529. doi:10.1146/annurev.fluid.34.090501.094913

[2] Wiltse, J. M., and Glezer, A., "Manipulation of Free Shear Flows Using Piezoelectric Actuators," *Journal of Fluid Mechanics*, Vol. 249, 1993, pp. 261–285. doi:10.1017/S002211209300117X

[3] Wiltse, J. M., and Glezer, A., "Direct Excitation of Small-Scale Motions in Free Shear Flows," *Physics of Fluids*, Vol. 10, 1998, pp. 2026–2036. doi:10.1063/1.869718

[4] Raman, G., Khanafseh, S., Cain, A. B., and Kerschen, E., "Development of High Bandwidth Powered Resonance Tube Actuators with Feedback Control," *Journal of Sound and Vibration*, Vol. 269, Nos. 3–5, 2004, pp. 1031–1062. doi:10.1016/S0022-460X(03)00212-8

[5] Kastner, J., and Samimy, M., "Development and Characterization of Hartmann Tube Fluidic Actuators for High-Speed Flow Control," *AIAA Journal*, Vol. 40, No. 10, 2002, pp. 1926–1934. doi:10.2514/2.1541

[6] Gregory, J. W., and Sullivan, J. P., "Characterization of Hartmann Tube Flow with Porous Pressure-Sensitive Paint," AIAA 33rd Fluid Dynamics Conference, AIAA Paper 2003-3713, Orlando, FL, 2003.

[7] Enloe, C. L., McLaughlin, T. E., VanDyken, R. D., Kachner, K. D., Jumper, E. J., and Corke, T. C., "Mechanisms and Responses of a Single Dielectric Barrier Plasma Actuator: Plasma Morphology," *AIAA Journal*, Vol. 42, No. 3, 2004, pp. 589–594. doi:10.2514/1.2305

[8] Corke, T. C., Post, M. L., and Orlov, D. M., "SDBD Plasma Enhanced Aerodynamics: Concepts, Optimization, and Applications," *Progress in Aerospace Sciences*, Vol. 43, Nos. 7–8, 2007, pp. 193–217. doi:10.1016/j.paerosci.2007.06.001

[9] Moreau, E., "Airflow Control by Non-Thermal Plasma Actuators," *Journal of Physics D: Applied Physics*, Vol. 40, No. 3, 2007, pp. 605–636. doi:10.1088/0022-3727/40/3/S01

[10] Crittenden, T. M., Warta, B. J., and Glezer, A., "Characterization of Pulsed Combustion Powered Actuators for Flow Control," 3rd AIAA Flow Control Conference, AIAA Paper 2006-2864, San Francisco, 2006.

[11] Rajendar, A., Crittenden, T. M., and Glezer, A., "Characterization of the Internal Flow Dynamics of Combustion Powered Actuators," 4th AIAA Flow Control Conference, AIAA Paper 2008-3760, Seattle, WA, 2008.

[12] Cybyk, B. Z., Simon, D. H., Land, H. B. III, Chen, J., and Katz, J., "Experimental Characterization of a Supersonic Flow Control Actuator," 44th AIAA Aerospace Sciences Meeting and Exhibit, AIAA Paper 2006-478, Reno, NV, 2006.

[13] Magill, J. C., and McManus, K. R., "Exploring the Feasibility of Pulsed Jet Separation Control for Aircraft Configurations," *Journal of Aircraft*, Vol. 38, No. 1, 2001, pp. 48–56. doi:10.2514/2.2733

[14] Chiekh, M. B., Bera, J. C., Michard, M., Comte-Bellot, G., and Sunyach, M., "Control of a Plane Jet by Fluidic Wall Pulsing," *AIAA Journal*, Vol. 41, No. 5, 2003, pp. 972–975. doi:10.2514/2.2036

[15] Rao, N. M., Feng, J., Burdisso, R. A., and Ng, W. F., "Experimental Demonstration of Active Flow Control to Reduce Unsteady Stator-Rotor Interaction," *AIAA Journal*, Vol. 39, No. 3, 2001, pp. 458–464. doi:10.2514/2.1327

[16] Saric, W. S., and Reed, H. L., "Effect of Suction and Weak Mass Injection on Boundary-Layer Transition," *AIAA Journal*, Vol. 24, No. 3, 1986, pp. 383–389. doi:10.2514/3.9278

[17] Miller, D. N., Yagle, P. J., Bender, E. E., Smith, B. R., and Vermeulen, P. J., "A Computational Investigation of Pulsed Injection into a Confined, Expanding Crossflow," 31st AIAA Fluid Dynamics Conference and Exhibit, AIAA Paper 2001-3026, Anaheim, CA, 2001.

[18] Yagle, P. J., Miller, D. N., Bender, E. E., Smith, B. R., and Vermeulen, P. J., "A Computational Investigation of Pulsed Ejection," 1st AIAA Flow Control Conference, AIAA Paper 2002-3278, St. Louis, MO, 2002.

[19] Viets, H., "Flip-Flop Jet Nozzle," *AIAA Journal*, Vol. 13, No. 10, 1975, pp. 1375–1379. doi:10.2514/3.60550

[20] Morris, N. M., *An Introduction to Fluid Logic*, McGraw–Hill, London, 1973, pp. 58–66.

[21] Kirshner, J. M., and Katz, S., *Design Theory of Fluidic Components*, Academic Press, New York, 1975.

[22] Raman, G., Rice, E. J., and Cornelius, D. M., "Evaluation of Flip-Flop Jet Nozzles for Use as Practical Excitation Devices," *Journal of Fluids Engineering*, Vol. 116, No. 3, 1994, pp. 508–515. doi:10.1115/1.2910306

[23] Coanda, H., "Device for Deflecting a Stream of Elastic Fluid Projected into an Elastic Fluid," U.S. Patent 2,052,869, Sept. 1936.

[24] Metral, A., "Sur un Phenomene de Deviation des Vienes Fluides et Ses Applications (Effet Coanda)," *Proceedings of the 5th International Congress for Applied Mechanics*, Wiley, New York, and Chapman & Hall, London, 1939.

[25] Stouffer, R. D., "Liquid Oscillator Device," U.S. Patent 4,508,267, April 1985.

[26] Beale, R. B., and Lawler, M. T., "Development of a Wall Attachment Fluidic Oscillator Applied to Volume Flow Metering," *Flow: Its Measurement and Control in Science and Industry*, Vol. 1, Instrument Society of America, Pittsburgh, PA, 1974, pp. 989–996.

[27] Beale, R. B., *The Design of a Liquid Fluidic Reaction Jet System*, M.S. Thesis, Dept. of Mechanical Engineering, Massachusetts Inst. of Technology, Cambridge, MA, 1969.

[28] Wang, H., Beck, S. B. M., G. H. Priestman, and Boucher, R. F., "Fluidic Pressure Pulse Transmitting Flowmeter," *Chemical Engineering Research and Design*, Vol. 75, No. 4, 1997, pp. 381–391. doi:10.1205/026387697523840

[29] Raman, G., Raghu, S., and Bencic, T. J., "Cavity Resonance Suppression Using Miniature Fluidic Oscillators," 5th AIAA Aeroacoustics Conference, AIAA Paper 99-1900, Seattle, WA, 1999; also NASA TM-1999-209074, 1999.

[30] Raghu, S., and Raman, G., "Miniature Fluidic Devices for Flow Control," ASME Fluids Engineering Division Summer Meeting, American Society of Mechanical Engineers, Paper FEDSM 99-7526, 1999.

[31] Raman, G., Packiarajan, S., Papadopoulos, G., Weissman, C., and Raghu, S., "Jet Thrust Vectoring Using a Miniature Fluidic Oscillator," *Proceedings of the ASME Fluids Engineering Division Summer Meeting*, Vol. 1, American Society of Mechanical Engineers, New York, 2001, pp. 903–913.

[32] Raman, G., Hailye, M., and Rice, E. J., "Flip-Flop Jet Nozzle Extended to Supersonic Flows," *AIAA Journal*, Vol. 31, No. 6, 1993, pp. 1028–1035. doi:10.2514/3.11725

[33] Raman, G., "Using Controlled Unsteady Fluid Mass Addition to Enhance Jet Mixing," *AIAA Journal*, Vol. 35, No. 4, 1997, pp. 647–656. doi:10.2514/2.185

[34] Gregory, J. W., Sullivan, J. P., and Raghu, S., "Visualization of Jet Mixing in a Fluidic Oscillator," *Journal of Visualization*, Vol. 8, No. 2, 2005, pp. 169–176.

[35] Gregory, J. W., Sullivan, J. P., Raman, G., and Raghu, S., "Characterization of the Microfluidic Oscillator," *AIAA Journal*, Vol. 45, No. 3, 2007, pp. 568–576. doi:10.2514/1.26127

[36] Tesar, V., Hung, C.-H., and Zimmerman, W. B., "No-Moving-Part Hybrid-Synthetic Jet Actuator," *Sensors and Actuators A (Physical)*, Vol. 125, No. 2, 2006, pp. 159–169. doi:10.1016/j.sna.2005.06.022

[37] Tesar, V., Travnicek, Z., Kordik, J., and Randa, Z., "Experimental Investigation of a Fluidic Actuator Generating Hybrid-Synthetic Jets," *Sensors and Actuators A (Physical)*, Vol. 138, No. 1, 2007, pp. 213–220. doi:10.1016/j.sna.2007.04.064

[38] Tesar, V., "Configurations of Fluidic Actuators for Generating Hybrid-Synthetic Jets," *Sensors and Actuators A (Physical)*, Vol. 138, No. 2, 2007, pp. 394–403. doi:10.1016/j.sna.2007.05.027

[39] Arwatz, G., Fono, I., and Seifert, A., "Suction and Oscillatory Blowing Actuator Modeling and Validation," *AIAA Journal*, Vol. 46, No. 5, 2008, pp. 1107–1117. doi:10.2514/1.30468

[40] Lucas, N., Taubert, L., Woszidlo, R., Wygnanski, I., and McVeigh, M.

A., "Discrete Sweeping Jets as Tools for Separation Control," 4th AIAA Flow Control Conference, AIAA Paper 2008-3868, Seattle, WA, 2008.
[41] Cerretelli, C., and Gharaibah, E., "An Experimental and Numerical Investigation on Fluidic Oscillators for Flow Control," 37th AIAA Fluid Dynamics Conference and Exhibit, AIAA Paper 2007-3854, Miami, FL, 2007.
[42] Cerretelli, C., Gharaibah, E., Toplack, G., Gupta, A., and Wuerz, W., "Unsteady Separation Control for Wind Turbine Applications at Full Scale Reynolds Numbers," 47th AIAA Aerospace Sciences Meeting and Exhibit, AIAA, Paper 2009-380, Orlando, FL, 2009.
[43] Miller, W. V., "Experimental Feasibility Study of an Analog Electrical-to-Fluidic Transducer," *IEEE Transactions on Industrial Electronics and Control Instrumentation (IECI-16)*, Inst. of Electrical and Electronics Engineers, New York, 1969, pp. 50–58.
[44] Tesar, V., "The Guided Jet Principle," *Fluidics Quarterly*, Vol. 3, No. 4, 1971, pp. 77–99.
[45] Taft, C. K., and Herrick, B. M., "A Proportional Electro-Fluidic Pneumatic Valve Design," *20th Anniversary of Fluidics Symposium*, American Society of Mechanical Engineers, New York, 1980, pp. 1–7.
[46] Taft, C. K., and Herrick, B. M., "A Proportional Piezoelectric Electro-Fluidic Pneumatic Valve Design," *Journal of Dynamic Systems, Measurement, and Control*, Vol. 103, No. 4, 1981, pp. 361–365. doi:10.1115/1.3139676
[47] Chen, R., and Lucas, G. G., "Investigation into the Use of Piezo-Fluidic Combined Units as Fuel Injectors for Natural Gas Engines," *Proceedings of the 1996 International Fall Fuels & Lubricants Meeting & Exposition*, Vol. 1208, SAE Special Publications, Warrendale, PA, Oct. 1996, pp. 123–134.
[48] Chen, R., "Piezo-Fluidic Gaseous Fuel MPI System for Natural Gas Fuelled IC Engines," *JSME International Journal, Series B (Fluids and Thermal Engineering)*, Vol. 44, No. 1, 2001, pp. 158–165. doi:10.1299/jsmeb.44.158
[49] Gregory, J. W., Gnanamanickam, E. P., Sullivan, J. P., and Raghu, S., "Variable-Frequency Fluidic Oscillator Driven by Piezoelectric Devices," 43rd AIAA Aerospace Sciences Meeting, AIAA Paper 2005-0108, Reno, NV, 2005.
[50] Gregory, J. W., Ruotolo, J. C., Byerley, A. R., and McLaughlin, T. E., "Switching Behavior of a Plasma-Fluidic Actuator," 45th AIAA Aerospace Sciences Meeting and Exhibit, AIAA Paper 2007-0785, Reno, NV, 2007.
[51] Culley, D., "Variable Frequency Diverter Actuation for Flow Control," 3rd AIAA Flow Control Conference, AIAA Paper 2006-3034, San Francisco, 2006.
[52] Feikema, D., and Culley, D., "Computational Fluid Dynamic Modeling of a Fluidic Actuator for Flow Control," 46th AIAA Aerospace Sciences Meeting and Exhibit, AIAA Paper 2008-0557, Reno, NV, 2008.
[53] Settles, G. S., *Schlieren & Shadowgraph Techniques: Visualizing Phenomena in Transparent Media*, Springer, New York, 2006.
[54] Bell, J. H., Schairer, E. T., Hand, L. A., and Mehta, R. D., "Surface Pressure Measurements Using Luminescent Coatings," *Annual Review of Fluid Mechanics*, Vol. 33, 2001, pp. 155–206. doi:10.1146/annurev.fluid.33.1.155
[55] Liu, T., and Sullivan, J. P., *Pressure and Temperature Sensitive Paints*, Springer, New York, 2005.
[56] Gregory, J. W., Asai, K., Kameda, M., Liu, T., and Sullivan, J. P., "A Review of Pressure-Sensitive Paint for High-Speed and Unsteady Aerodynamics," *Proceedings of the Institution of Mechanical Engineers, Part G (Journal of Aerospace Engineering)*, Vol. 222, No. 2, 2008, pp. 249–290. doi:10.1243/09544100JAERO243
[57] Gregory, J. W., "Porous Pressure-Sensitive Paint for Measurement of Unsteady Pressures in Turbomachinery," 42nd AIAA Aerospace Sciences Meeting, AIAA Paper 2004-0294, Reno, NV, 2004.
[58] Gregory, J. W., and Sullivan, J. P., "Effect of Quenching Kinetics on Unsteady Response of Pressure-Sensitive Paint," *AIAA Journal*, Vol. 44, No. 3, 2006, pp. 634–645. doi:10.2514/1.15124
[59] Gregory, J. W., Sullivan, J. P., Wanis, S., and Komerath, N. M., "Pressure-Sensitive Paint as a Distributed Optical Microphone Array," *Journal of the Acoustical Society of America*, Vol. 119, No. 1, 2006, pp. 251–261. doi:10.1121/1.2140935

A. Naguib
Associate Editor